Reducing heavy rare earth elements by combining permanent magnets in IPM motors

Shunsuke Takahashi [1)] **Yutaka Sasaki** [1)]

1) Hino Motors, Ltd.3-1-1, Hino-dai, Hino-shi, Tokyo, Japan
E-mail: shunsuke.takahashi@hino.co.jp

ABSTRACT: The technique of combining two types of magnets, referred to as the joined magnet, was investigated as a method to reduce the amount of heavy rare earth elements used in high coercivity magnets for IPM motors. In this approach, the magnets in the rotor were divided, and some parts were replaced with low coercivity (less heavy rare earth elements) magnets. It was found that motor performance, such as torque and efficiency, could be maintained. This technique suggests that simply replacing the magnets used in conventional motors can reduce the amount of heavy rare earth elements while maintaining demagnetization resistance and motor performance.

1. INTRODUCTION

In recent years, the interior permanent magnet motor (IPM motor) has become the mainstream for drive motors used in electric vehicles. Neodymium (Nd) sintered magnets with high coercivity (Hcj) are commonly used for magnets embedded in the rotor.

However, to enhance the Hcj of sintered magnets, heavy rare earth elements like dysprosium (Dy) and terbium (Tb) are added. These elements are at risk of resource depletion. Consequently, various technologies for reducing the use of heavy rare earth elements have been developed thus far.

Among these heavy rare earth reduction technologies, the most representative are magnets that do not rely on heavy rare earth elements, produced by magnet manufacturers. For example, hot-deformed magnets[(1)] achieve high coercivity without the addition of Dy. However, their coercivity is not as high as that of high-grade sintered magnets with Dy or Tb. Additionally, cost is a consideration compared to sintered magnets.

On the other hand, motor manufacturers and automobile manufacturers have focused on methods that adjust coercivity in accordance with the uneven magnetic field within the motor. In IPM motors, the magnets at the corners or ends are often exposed to stronger demagnetizing fields than those in the center. Therefore, some technologies have been developed to increase the coercivity only at the corners or ends of the magnets. For example, the partial diffusion method[(2)] is a technology that concentrates the diffusion of heavy rare earth elements at the corners of the magnets. By keeping the concentration of heavy rare earth elements low in areas where high coercivity is not needed, the overall use of heavy rare earth elements in the magnet is reduced. Another example is joined magnets[(3, 4)], where sintered magnets with high coercivity and low coercivity are joined together. This approach uses different sintered magnets for areas that require high coercivity and those that do not. Additionally, in some commercial motors, the Dy concentration in magnets placed on the inner periphery of the rotor is lower than those on the outer periphery.

As mentioned above, various approaches focusing on the uneven magnetic field within the rotor have been conducted, but these are fundamentally technologies applied when developing new motors. The development of new motors requires time and cost. Therefore, replacing the magnets of already mass-produced motors is a simpler way to reduce the use of heavy rare earth elements. However, there are few studies that have verified whether there is no performance difference when replacing the magnets of existing motors while keeping other conditions unchanged.

In this study, we focused on joined magnets and aimed to verify that replacing only the magnets does not affect motor performance.

2. EXPERIMENTAL METHODS

2.1. Material of magnets

To ensure that the replacement of magnets does not affect motor performance, the material selection for joined magnets aimed to (i) secure demagnetization resistance and (ii) maintain the residual magnetic flux density (Br) unchanged.

(i) Securing demagnetization resistance: In order to secure demagnetization resistance, preliminary magnetic field analysis was conducted on the motor to be used in the experiment described later. The analysis results are shown in Figure 1. The magnetic field is uneven, and particularly strong demagnetizing fields are generated at both end corners of the magnet.

Based on the analysis, the dimensions and materials of the joined magnet were determined, as illustrated in Figure 2. Here, the "Single magnet" refers to a state where one type of magnet (magnet A) is embedded in each slot of the rotor. In contrast, “Joined magnet” uses two types of magnets (magnets A and B) in the slots. In the case of “Joined magnet”, magnet A is used at both ends, while magnet B is used in the center. Magnet B contains fewer heavy rare earth elements and has lower coercivity than magnet A. The dimensions of the magnets shown in Figure 2 represent the total length, including the surface plating thickness (approximately 15–20 μm). Additionally, the joined magnet dimensions account for the adhesive thickness (approximately 0.1 mm) between magnet A and magnet B. Although fine control of the adhesive thickness is challenging, a metal frame corresponding to the dimensions shown in Figure 2 was prepared. After applying the adhesive, the adhesive was dried within the metal frame to achieve the desired dimensions.

It is noted that the main components and magnetic properties of magnets A and B are shown in Tables 1 and 2. In the joined magnet, the volume ratio of magnets A and B is approximately 1:1. When considering the joined magnet as a single bulk material, the apparent Dy concentration is 4.92%. Since the Dy concentration of the single magnet is 6.76%, the joined magnet reduces the Dy concentration by 1.84 points.

(ii) Maintaining Br: In order to equalize the magnetic flux density of the joined magnet with that of the single magnet, a magnet with exactly the same residual magnetic flux density (Br) as magnet A should have been placed at the center of the joined magnet. However, since such a magnet was not available, a magnet with a similar Br (magnet B) was selected. Although the Br of magnets A and B differ, the adhesive at the contact surfaces and the plating on the surface have very little magnetic force. Considering these factors, the apparent Br of the joined magnet is approximately 1.28 T, which is roughly within the manufacturing variation range of magnet A. Therefore, the apparent magnetic flux density of the joined magnet is approximately equivalent to that of a single magnet.

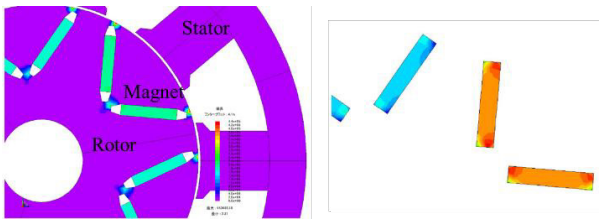

Fig. 1 Pre-analyzed magnetic field distribution for the motor (left) and magnets (right).

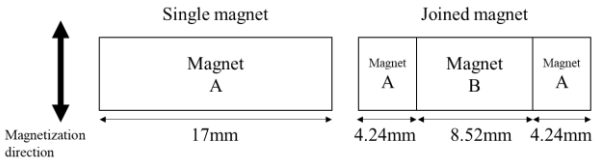

Fig.2 Schematic of single and joined magnets (length includes surface treatment and adhesive thickness).

Table 1 Compositions of Rare Earth Elements in Magnets A and B (mass%).

	Nd	Pr	Dy	Tb
Magnet A	24.9	<0.10	6.76	<0.05
Magnet B	28.4	0.10	3.07	<0.05

Table 2 Magnetic properties of Magnet A and B.

	Temperature [°C]	Residual flux density, Br [T]	Coercivity, Hcj [kA/m]
Magnet A	20	1.25	1989
	100	1.17	1209
Magnet B	20	1.32	1289
	100	1.23	634

2.2. Trial motor

Figure 3 shows the appearance of the prototype stator, single magnet rotor, and joined magnet rotor. Additionally, Table 3 gives the motor specifications. Two rotors were prepared, one with a single magnet and the other with a joined magnet. For the joined magnet, magnets A and B were bonded with an adhesive before being magnetized and inserted into the rotor. The single magnet was also magnetized before being inserted into the rotor.

In order to confirm that the Br of the single magnet and joined magnet are equal, the surface magnetic flux density of the rotor's outer circumference was measured. Figure 4 shows the circumferential surface magnetic flux density distribution at an axial height of 0 mm. The magnetic flux density at the peak position is larger in the single magnet rotor, with a difference of approximately 16% at the 20° peak position. Figure 5 shows the

height direction surface magnetic flux density distribution (the circumferential position is 0° as shown in Figure 4). The height direction magnetic flux density distributions are generally equal, but near 0 mm, the single magnet rotor has a larger magnetic flux density. The total magnetic flux of the entire outer surface of the rotor was calculated from the magnetic flux density (absolute value) at each position. The single magnet rotor was 6.92×10^{-4} Wb, and the joined magnet rotor was 6.99×10^{-4} Wb. The joined magnet rotor was 1% larger in total magnetic flux.

From the above, it is considered that the surface magnetic flux densities of the single magnet rotor and joined magnet rotor are generally equal, with slight differences likely due to manufacturing variations of the magnets and rotor core.

Fig. 3 Stator (left), single magnet rotor (middle), and joined magnet rotor (right).

Table 3 Motor Specifications.

Rated output	1.6 kW
Rated torque	5.0 Nm
Max. RPM	6000 rpm
Rated RPM	3000 rpm
Number of slots	9
Number of poles	6
Stack length	30 mm
Stator outer diameter	160 mm
Rotor outer diameter	94.6 mm
Cooling type	Natural air cooling
Core material	35A300

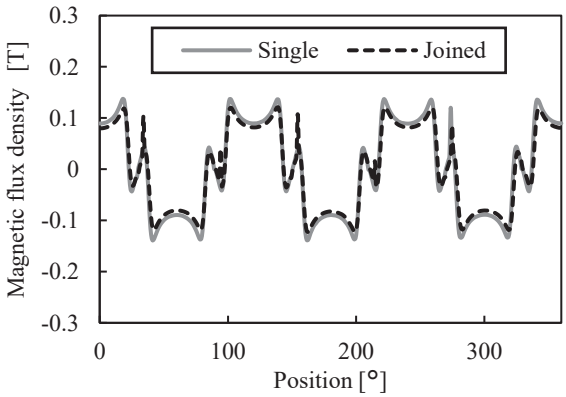

Fig. 4 Magnetic flux density distribution in circumferential direction on outer surface of rotor (measured at 0 mm height).

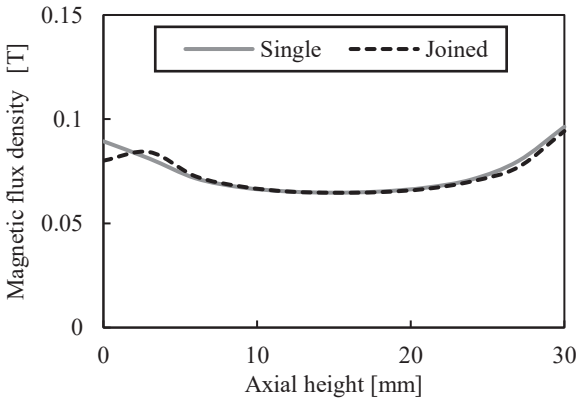

Fig. 5 Magnetic flux density distribution in axial direction on the outer surface of the rotor (circumferential direction: 0° in Fig. 4).

2.3. Verification of principle feasibility

The feasibility of the joined magnet was confirmed through simulations using JMAG Designer 19.1. Table 4 gives the driving conditions assumed in the calculations. The driving conditions were determined based on a rated torque of 5.0 Nm at 3000 rpm and a maximum speed of 6000 rpm at 1.6 Nm.

Table 4 Motor drive conditions in the calculations.

Magnet	Case No.	RPM [rpm]	Target torque [Nm]	Magnet Temperature [°C]
Single	1	3000	5.0	100
	2	6000	1.6	100
Joined	3	3000	5.0	100
	4	6000	1.6	100

2.4. Experimental verification

In order to experimentally verify the feasibility of the joined magnet, motor bench tests were conducted under the driving conditions shown in Table 5. Though different rotor cores were used for the single magnet and the joined magnet, the same stator core was used for both.

It should be noted that when planning the experiment, the target magnet temperature for Cases 6, 8, 10, and 12 was originally set to 100°C. However, due to equipment limitations, the maximum achievable temperature was 70°C. Consequently, the temperature was adjusted to 70°C.

In the cases where the magnet temperature was 70°C (Cases 6, 8, 10 and 12), the rotors were heated with hot air from a heater applied in the axial direction. The magnet temperature was measured before the test using the thermocouple attached to the center of the magnet surface. After confirming that the magnet temperature reached 70°C, it was maintained for a sufficient time.

Then, the thermocouple was removed before driving the motor. Therefore, the magnet temperature of 70°C is the temperature just before the test and was not measured during the test.

Table 5 Motor drive conditions in the experiments.

Magnet	Case No.	RPM [rpm]	Target Torque [Nm]	Target Magnet Temperature [°C]
Single	5	3000	5.0	R.T.
	6	3000	5.0	70
	7	6000	1.6	R.T.
	8	6000	1.6	70
Joined	9	3000	5.0	R.T.
	10	3000	5.0	70
	11	6000	1.6	R.T.
	12	6000	1.6	70

The irreversible demagnetization of the magnet was confirmed as follows. The no-load induced voltages between terminals (U–V, V–W and W–V) were measured before and after each test. If the voltage remained unchanged, it was determined that irreversible demagnetization did not occur. The no-load induced voltage measurements were conducted at room temperature for all cases. For Cases 6, 8, 10 and 12 (where the magnet temperature was 70°C), the induced voltages were measured before heating and after the temperature had returned to room temperature following the test.

The motor performance of single magnet and joined magnet was evaluated in terms of the current required to achieve the target torque and motor efficiency, copper loss and iron loss. The motor efficiency, copper loss, and iron loss were determined as follows.

First, the total loss (L_{total}) was obtained from Equation (1). Here, $P_{calculated}$ is the theoretical output derived from torque and rotational speed in each case, as calculated using Equation (2). $P_{measured}$ is the value read from the power meter. T is the value of average torque and r is the rotational speed. The units of loss and output are W, torque is in Nm, and rotational speed is in rpm. Subsequently, the efficiency (E) was determined by Equation (3).

$$L_{total} = P_{calculated} - P_{measured} \quad \text{...Eq. (1)}$$

$$P_{calculated} = T \times r \times 2\pi / 60 \quad \text{...Eq. (2)}$$

$$E = P_{measured} / P_{calculated} \quad \text{...Eq. (3)}$$

The copper loss (L_{copper}) was calculated by the current (I) and the electrical resistance of the total coil (R_{coil}) from Equation (4). The unit of current is Arms and resistance is in Ω. Here, in Equation (4), R_{coil} was determined by the value at room temperature and the temperature dependence of copper electrical resistance.

$$L_{copper} = I^2 \times R_{coil} \quad \text{...Eq. (4)}$$

Finally, the iron loss (L_{iron}) was determined from Equation (5).

$$L_{iron} = L_{total} - L_{copper} \quad \text{...Eq. (5)}$$

3. RESULTS AND DISCUSSIONS

3.1. Verification of principle feasibility

Figure 6 shows the magnetic field distribution in the magnets in Cases 1 and 3. Table 6 gives the maximum magnetic field in the magnets. The magnetic field in the magnet is sufficiently lower than the Hcj of magnets A and B at 100°C (shown in Table 2), suggesting that irreversible demagnetization does not occur.

Table 7 gives the summary of the calculation results for Cases 1–4. Figure 7 shows the efficiency, copper loss and iron loss obtained from the calculation. The performances of the single magnet and the joined magnet are generally equivalent (between Case 1 and 3, or between Case 2 and 4). From the above, it is considered that replacing only the magnets from single magnet to joined magnet does not change the motor performance in principle.

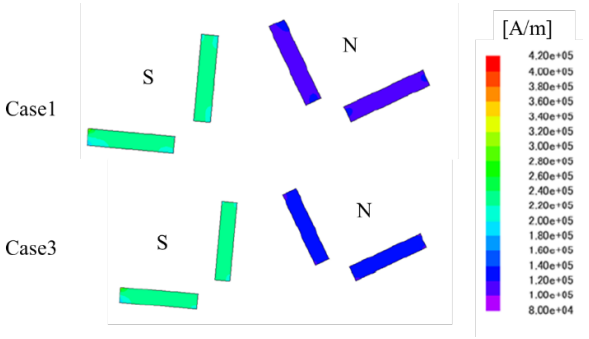

Fig. 6 The magnetic field distribution in the magnet obtained from the calculations in cases 1 and 3.

Table 6 Maximum magnetic field in the magnet in case1–4.

Magnet	Case No.	Maximum magnetic field [kA/m]	
		in Magnet A	in Magnet B
Single	1	414	-
	2	239	-
Joined	3	413	226
	4	248	207

Table 7 Summary of the calculation results.

Magnet	Case No.	Average torque, [Nm]	Magnet temperature [°C]	Current, [Arms]	d-axis inductance, L_d [H]	q-axis inductance, L_q [H]	Copper loss [W]	Iron loss [W]				
								total	Rotor		Stator	
									hysteresis loss	eddy current loss	hysteresis loss	eddy current loss
Single	1	4.68	100	11.54	0.0020	0.0037	22.74	20.12	0.88	3.01	7.59	8.64
	2	1.50	100	6.640	0.0021	0.0040	7.53	28.82	0.66	4.33	7.48	16.35
Joined	3	4.76	100	11.54	0.0020	0.0037	22.74	20.43	0.89	3.03	7.69	8.83
	4	1.53	100	6.640	0.0021	0.0039	7.53	29.99	0.70	4.49	7.82	16.98

Table 8 Summary of the experimental results.

Magnet	Case No.	Average torque, T [Nm]	Magnet temperature [°C]	Coil temperature [°C]	Current, I [Arms]	d-axis inductance, L_d [H]	q-axis inductance, L_q [H]	Copper loss, L_{copper} [W]	Iron loss, $L_{iron,}$ [W]
Single	5	5.0	23	56	12.01	0.0015	0.0024	61.50	31.15
	6	4.94	75	71	12.01	0.0015	0.0025	64.89	35.93
	7	1.6	23	32	6.52	0.0015	0.0028	16.56	9.68
	8	1.55	72	60	6.52	0.0016	0.0027	18.28	13.93
Joined	9	5.0	23	56	12.26	0.0015	0.0024	64.51	28.18
	10	4.90	71	64	12.26	0.0021	0.0024	65.89	24.45
	11	1.59	23	42	7.79	0.0016	0.0021	24.53	6.44
	12	1.57	71	61	7.79	0.0016	0.0023	26.10	6.82

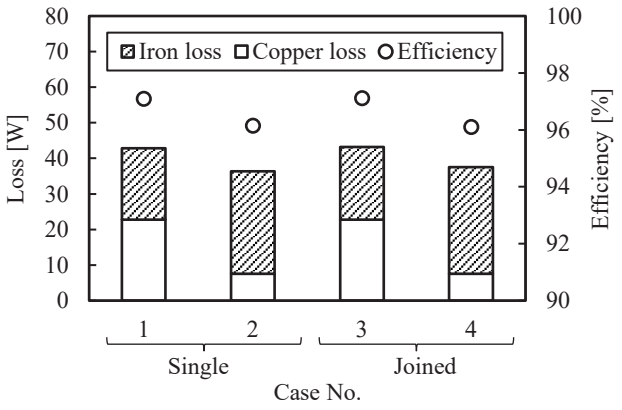

Fig. 7 Efficiency, copper loss and iron loss obtained from the calculation.

3.2. Experimental Verification

Table 8 gives the summary of the motor bench test results. The following paragraphs explain the confirmation of demagnetization through the measurement of no-load induced voltage and compare the motor performances between single and joined magnet.

Figure 8 shows the no-load induced voltage between the U–V terminals before and after the tests in Cases 6, 8, 10 and 12. The fact that the no-load induced voltage remained equal before and after the tests indicates that irreversible demagnetization did not occur. The same was true for the V–W and W–U terminals. Additionally, in all experimental cases of Case 5–12, the no-load induced voltages remained unchanged before and after the tests.

Comparing the single magnet and joined magnet shown in Figure 8, the joined magnet has a lower induced voltage. The difference is 3–5%, which can be attributed to the manufacturing variations of the motor mentioned in Section 2.2.

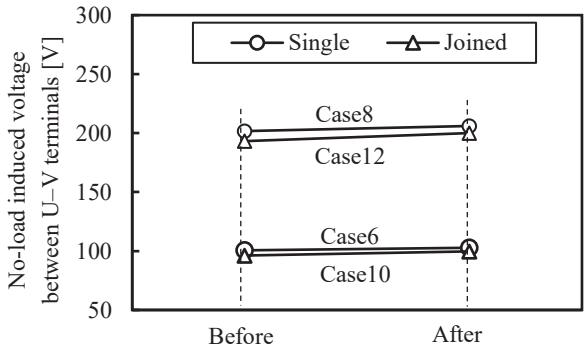

Fig. 8 No-load induced voltage between U and V terminals before and after Cases 6, 8, 10 and 12.

Figure 9 shows the current and torque. The relationships between current and torque are generally equivalent, but in the tests around 1.5 Nm, the joined magnet required more current. This is believed to be due to the lower no-load induced voltage of the joined magnet, as mentioned in Figure 8.

Figure 10 shows the motor efficiency, copper loss and iron loss measured in the experiments. Although these values for the single magnet and the joined magnet are roughly equivalent, there is a slight tendency for the joined magnet to exhibit higher

copper losses and lower iron losses. This can be attributed to the no-load induced voltage. As mentioned in Figures 8 and 9, the joined magnet has a lower induced voltage, which requires more current to produce the same torque as the single magnet, resulting in higher copper losses.

Regarding iron loss, several previous studies[5, 6] have reported that dividing the magnet can reduce eddy current loss. However, in this study, although the experimental analysis is not sufficient, the calculation results in Table 7 show that the rotor eddy current loss of the joined magnet is slightly larger than that of the single magnet. Additionally, in Cases 1–4, the rotor eddy current loss is about 15% of the total iron loss of the motor, indicating a small impact. Therefore, the reduction in iron loss of the joined magnet shown in Figure 10 is probably not due to this factor.

From the above, it can be concluded that while there are differences due to manufacturing variations, the motor performances are generally equivalent.

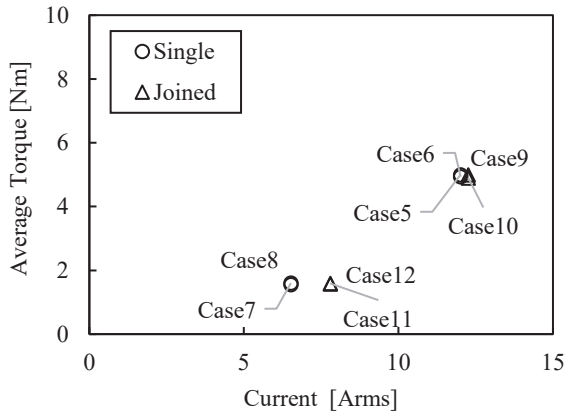

Fig. 9 Average torque and current measured in the experiments.

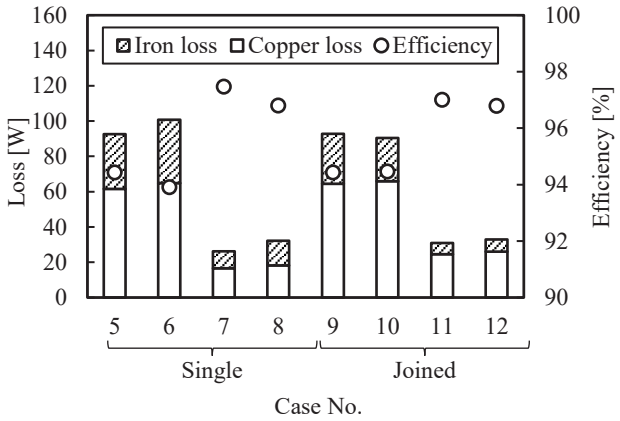

Fig. 10 Efficiency, copper loss and iron loss measured in the experiments.

4. CONCLUSIONS

It was confirmed through simulations and experiments that replacing single magnets with joined magnets results in equivalent motor performance.

In this case, the Dy concentration in the single magnet was 6.76%, while in the joined magnet, it was apparently 4.92%. This represents a reduction of 1.84 percentage points.

It is considered that by replacing only the magnets of existing motors, it is possible to reduce the amount of heavy rare earth elements while maintaining motor performances.

REFERENCES

(1) Keiko Hioki *et al*., DENKI-SEIKO, vol.86, No.2, p.p.83–92 (2016)

(2) Takehiro Miyoshi *et al*., Honda R&D Technical Review, vol. 24, No.2, p.p. 61-66, 2012.

(3) Toyota Motor Corporation, Keiji Kaneda, Japan Patent Kokai 2006-261433(2006.09.28).

(4) Sankyo Seiki Mfg. Co., Ltd., M. Ishikawa *et al*., Japan Patent Kokai 2001-110617(2001.04.20).

(5) Masato Sagawa *et al.*, "Permanent Magnets: Materials Science and Applications", AGNE Gijutsu Center Inc., Tokyo,2007, p.p.363–364

(6) Htoshi Yamamoto *et al*., "Coercivity of permanent magnets and related technical challenges", Neoji-consul, Japan, 2024 p.p.76–79